

- Congress on Computation intelligence,pp.69-73,1998.
28. Takahashi, Masato, and Hajime Kita. "A crossover operator using independent component analysis for real-coded genetic algorithms." *Evolutionary Computation*, 2001. Proceedings of the 2001 Congress on. Vol. 1. IEEE, 2001.
 29. Zhi-Feng Hao,Zhi-Gang Wang,HanHuang,A Particle Swarm Optimization Algorithm With Crossover Operator Proceedings of the 6th international conference on Machine Learning and Cybernetics ,Hong Kong ,19-22 August 2007.
 30. Chen, Stephen. "Particle swarm optimization with pbestcrossover." *Evolutionary Computation (CEC)*, 2012 IEEE Congress on. IEEE, 2012.
 31. Qinghai bai, China"Analysis of Particle Optimization Algorithm"computer and information science (CCSE), Vol. 3, No. 1, Februry 2010.
 32. Q.H. Wu, Y.J.Cao, and J.Y. Wen. Optimal reactive power dispatch using an adaptive genetic algorithm. *Int. J. Elect. Power Energy Syst.* Vol 20. Pp. 563-569; Aug 1998.
 33. B. Zhao, C. X. Guo, and Y.J. CAO. Multiagent-based particle swarm optimization approach for optimal reactive power dispatch. *IEEE Trans. Power Syst.* Vol. 20, no. 2, pp. 1070-1078, May 2005.
 34. Mahadevan. K, Kannan P. S. "Comprehensive Learning Particle Swarm Optimization for Reactive Power Dispatch", *Applied Soft Computing*, Vol. 10, No. 2, pp. 641–52, March 2010.
 35. A.H. Khazali, M. Kalantar, "Optimal Reactive Power Dispatch based on Harmony Search Algorithm", *Electrical Power and Energy Systems*, Vol. 33, No. 3, pp. 684–692, March 2011.
 36. S. Sakthivel, M. Gayathri, V. Manimozhi, "A Nature Inspired Optimization Algorithm for Reactive Power Control in a Power System", *International Journal of Recent Technology and Engineering (IJRTE)* ,pp29-33 Volume-2, Issue-1, March 2013.
 37. Chaohua Dai, Weirong Chen, Yunfang Zhu, and Xuexia Zhang, "Seeker optimization algorithm for optimal reactive power dispatch," *IEEE Trans. Power Systems*, Vol. 24, No. 3, August 2009, pp. 1218-1231.
 38. J. R. Gomes and O. R. Saavedra, "Optimal reactive power dispatch using evolutionary computation: Extended algorithms," *IEE Proc.-Gener. Transm. Distrib..* Vol. 146, No. 6. Nov. 1999.
 39. IEEE, "The IEEE 30-bus test system and the IEEE 118-test system", (1993), <http://www.ee.washington.edu/trsearch/pstca/>.
 40. Jiangtao Cao, Fuli Wang and Ping Li, " An Improved Biogeography-based Optimization Algorithm for Optimal Reactive Power Flow" *International Journal of Control and Automation* Vol.7, No.3 (2014), pp.161-176.

Prediction of Efficiency for a Passive Flat Plate Collector for Water Desalination using Artificial Neural Network

Alex Okibe Edeoja Kuncy Kumadem Ikpambese
Department of Mechanical Engineering, University of Agriculture, Makurdi, Nigeria

The research is financed by the authors utilizing their teaching and research allowances.

Abstract

Artificial neural network was used for modeling and prediction of the efficiency of a passive flat plate collector for water desalination. An extensive experimental program design was undertaken on the collector to obtain the parameters required for the modeling. The neural model to predict the efficiency was developed based on groups of experiments carried out. Five (5) parameters: ambient, inlet fluid and outlet fluid temperatures, radiation, and aperture area of the collector were used as inputs into the network architecture of 5 [5]₁ 1 in predicting the efficiency. After series of network architectures were trained using different training algorithms such as Levenberg-Marquardt, Bayesian Regulation, Resilient Backpropagation using MATLAB 7.9.0 (R20096), the LM 5 [5]₁ 1 was selected as the most appropriate model. Prediction of the neural model exhibited reasonable correlation with the experimental collector efficiency. The predicted collector efficiency gave minimal MSE errors and higher correlation coefficients and Nash-Scutcliffe efficiency (NSE) indicating that the model was robust for predicting the efficiency of a passive flat plate collector for desalination of water.

Keywords: Collector efficiency, desalination, passive solar collector, artificial neural network, Nash-Scutcliffe efficiency, MSE error, modeling.

1. Introduction

Desalination is a proven technology that has been used for many years in areas with scarce water supplies. However, because of its relatively high cost, it is generally used only if fresh water supplies are limited. Water desalination technologies can be categorized on the basis of the energy used to run them, usually thermal or electric. There are also other technologies that rely on solar energy or combined electric and thermal energy. Each of these technologies has advantages and disadvantages, based on the quantity and quality of the required water and the location. Advances in desalination technology continue to make these processes more efficient. Recent investigations have focused on the use of renewable energy to provide the required power for the desalination processes, the most popular renewable energy source being solar energy. An emerging technology for smaller scale desalination system is the use of solar energy to evaporate fresh water, which is condensed on a cool surface and collected. Solar desalination systems are simple and easy to operate and maintained. They are also environmentally friendly because they do not require fossil fuels. In locations with abundant sunshine, solar desalination is a potentially viable option, especially for small scale plants in remote locations (Edeoja et al, 2009).

Solar thermal collector is a device for intercepting solar radiation, converting this radiation to heat in a fluid, and delivering the heated fluid for use. A flat collector consists of ; a dark flat-plate absorber of solar energy, a transparent cover that allows solar energy to pass through but reduces heat losses, a heat-transport fluid (air, antifreeze or water) flowing through tubes to remove heat from the absorber, and a heat insulation backing. The absorber consists of a thin absorber sheet (of thermally stable polymers, aluminium, steel or copper, to which a black or selective coating is applied) backed by a grid or coil of fluid tubing placed in an insulated casing with a glass or polycarbonate cover. Fluid is circulated through the tubing to transfer heat from the absorber to an insulated water tank. This may be achieved directly or through a heat exchanger. Some are also fabricated with a completely flooded absorber consisting of two sheets of metal stamped to produce a circulation zone (Kuhe, 2004).

The use of artificial neural network (ANN) in the field of engineering has widened rapidly. For instance the prediction of compressibility and oil absorption for gasket produced from palm kernel fibres was investigated by Ikpambese et al, (2012). Adnan et al (2005) used ANN to determine the properties of liquid and two phase boiling and condensing of two alternative refrigerant/absorbent couples (methanol/LiBr and methanol/LiCl). Zhang (2005) used a generalized ANN based correlation for predicting the mass flow rate of refrigerant through the capillary tube. Lolas and Olatunbosun, (2008) presented a neural network architecture that predicted the reliability performance of a vehicle at later stages of its life by using only information from a first inspection after the vehicle's prototype production. Application of ANN to predict the heat transfer rate of the wire-on-tube type heat exchanger was undertaken by Yasar (2003).

This study intends to predict the efficiency of a developed passive flat collector for water desalination using artificial neural network. The prediction of the efficiency of a developed passive flat collector for water desalination was based on the following inputs: (i) Atmospheric temperature, (ii) Temperature of the fluid

entering the collector, (iii) Temperature of the fluid leaving the collector, (iv) Radiation, and (v) Area of the collector against efficiency as the output

2. Materials and Methods

2.1 Description of the passive solar collector

The test rig consisted of a storage container of 35l capacity and the flat plate solar collector. The storage container was installed 150cm above the ground level in order to generate a potential difference for flow into the collector. The angle of tilt of the collector was 29.7°. The collectors' inlet was connected to the container tap through a hose with the aid of PVC gum and hose clip. Provision for measuring the temperature of the water in the container, at the collector inlet and outlet were made. Figures 1 and 2 described a schematic diagram and a photo respectively of the system.

2.2 Experimentation

The storage container was first filled with water to full capacity. The tap was then opened for water to flow by gravity down to the inlet pipe of the collector. A thermocouple was used to measure the temperatures of the water at the three points. The tap was regulated such that water flows through the collector at an average rate of about 0.00054litres/s so that it has a reasonable resident time within the black-coated copper coils of the collector thereby adsorbing more heat by conduction.

The temperature of the outer surface of the collector glazing was also measured. The procedure was repeated hourly from 10:00am to 4:00pm daily. The solar radiation values were measured using a solarimeter (sun meter). The collector efficiency was computed using equation (1) according to George (1980).

$$= \frac{Q_u}{I_t \times A_c} = F_R \times \tau \times \alpha - F_R \times U_L \left(\frac{t_i - t_a}{I_t} \right) \quad (1)$$

where Q_u = useful energy delivered by the collector (W), A_c = total collector area (m^2), I_t = solar energy received on the upper surface of the sloping collector structure (W/m^2), τ = fraction of incoming solar radiation that reaches the absorbing surface, transmissivity (dimensionless), α = fraction of solar energy reaching the surface that is absorbed, absorptivity (dimensionless), U_L = overall heat loss coefficient ($W/m^2 \cdot ^\circ C$), t_i = temperature of fluid entering the collector ($^\circ C$), t_a = atmospheric temperature ($^\circ C$), and F_R = heat removing factor (dimensionless).

2.3 Neural network Modeling

The adoption of the neural network for the prediction of efficiency of passive flat plate collector for water desalination was based on the experimental data. The following steps were employed for the modeling; (i) data generator, (ii) definition of ranges and distribution of training data set, (iii) data pre-processing, (iv) selection of training algorithms, (v) training the neural network and (vi) testing or predicting Gundu et al, (2013).

2.3.1 Input data and Output

The input data captured in the ANN modeling were: (i) Atmospheric temperature, (ii) Temperature of the fluid entering the collector, (iii) Temperature of the fluid leaving the collector, (iv) Radiation, and Area of the collector, totaling five parameters. The input parameters range S_{T1} - S_{T12} as shown on Table 1 were used for training the network while S_{P1} - S_{P6} were used for testing or prediction of the neural capabilities of the ANN. The values of data for the training the neural network was chosen outside the values of S_{P1} - S_{P6} obtained experimentally. The efficiency of the passive flat solar collector obtained from equation (1) was used as output as shown on Table 2. The data for the neural network modeling was obtained from six (6) groups of experimental data collected as samples and the working together of the influence of these five (5) inputs parameters on efficiency of the collector is shown on Fig 3.

2.3.2 Data pre-processing

Pre-processing of the input parameters was carried out before the neural network training. The experimental data involving the inputs were measured in different units; the data of different types have great difference. Such difference will decrease the convergence speed and accuracy within the network. The five (5) input parameters were scaled within the range of 0-1 using the relation given in equation (2) (Dragan, 2010):

$$I_{skat} = 1 + \left[\frac{I_{curr} - I_{Max}}{I_{Max} - I_{Min}} \right] \quad (2)$$

where I_{curr} is current input value, I_{Max} the maximum input value and I_{Min} the minimum input value. The output parameter collector' efficiency was presented to the network in percentage.

2.3.4 Network Training

A trial and error was used to find the best network's architecture for matching input/output relationship. The following networks architectures were investigated using MATLAB 7.9.0 (R20096); (i) one layered network 5 [1]₁ 1, 8 [5]₁ 1 (ii) two layered network 5 [3-2]₂ 1, 5 [4-2]₂ 1 (iii) three layered network 5 [5-4-2]₃ 1, 5 [4-3-2]₃ 1. The above networks architecture were trained using the following algorithms; Levenberg- Marquard (LM),

Bayesian Regulation (BR), Resilient Backpropagation (RB). The sigmoid function given in equation (3) was used between the input and the hidden layers.

$$f(x) = \frac{1}{1+e^{-x}} \quad (3)$$

and linear function $f(x) = x$ was used between the hidden and output layer, where x is the value of weight used.

3. Results and Discussion

Levenberg-Marquardt (LM) neural network model architecture of LM 5 [5]₁ 1 (5 neurons in the input layer, 1 hidden layers of 5 neurons and output layer of 1 neuron) was chosen for the modeling of efficiency of the collector, after series of training using different network architecture and algorithm described in section 2.4.4.

Training performance indicated values of correlation coefficient $R = 1.00$ at epoch 12 for training, $R = 0.8592$ for testing with validation checks was 6 at epoch 18 while the overall correlation coefficient (R) for training, testing, and validation was 0.94707. The neural model LM 5 [5]₁ 1, was chosen because its exhibited higher correlation coefficient for both training and testing compared with the other architecture and algorithm.

The neural model LM 5 [5]₁ 1 was used to predict the values of efficiency of the collector with MSE network errors between the predicted and experimental (real) are described in Tables 3 respectively. The correlation coefficient and Nash-Scutcliffe efficiency (NSE) were used to examine the strength of linear relationship between the predicted and experimental (real) values using the relation in equation (4) and (5) (Haghdadi et al, 2013; Mohanty et al, 2013) respectively.

$$R = \frac{\sum_{i=1}^N (E_i - \bar{E})(P_i - \bar{P})}{\sqrt{\sum_{i=1}^N (E_i - \bar{E})^2 \sum_{i=1}^N (P_i - \bar{P})^2}} \quad (4)$$

$$NSE = 1 - \frac{\sum_{i=1}^N (E_i - P_i)^2}{\sum_{i=1}^N (E_i - \bar{E}_i)^2} \quad (5)$$

where E is the sample of the experimental value, p is the sample of predicted value by an ANN model \bar{E} and \bar{P} are the mean value of E and P respectively, N is the number of sample.

Table 3 shows the values of the predicted and experimental (real) efficiency of the collector with their respective mean square errors, correlation coefficients and Nash-Scutcliffe efficiency (NSE). It was observed that the neural network prediction of efficiency of the collector was in agreement with the experimental (real) efficiency of the collector with minimal mean square errors of -0.0000195, 0.000000011, -0.00000000139, 0.0002912, 0.0065103, 0.000001340 and higher correlation coefficient and Nash-Scutcliffe efficiency of 1.0000, 1.0000, 1.0000, 1.0000, 1.0000, 1.0000, 1.0000, 0.9999, 1.0000, 1.0000, 1.0000, 1.0000 respectively. The values of the correlation coefficients were better compared with the values of 0.99997, 0.99999, 0.99997 and 0.99998 by Quan et al (2013). The slight disparity in some of the predicted and experimental could be attributed errors arising from calculation.

The quality of the prediction of the collector's efficiency was also shown taking into cognizance the following points (i) the quality of prediction of collector's efficiency against radiation (ii) collector's efficiency against temperature of the fluid entering the system. Fig. 4 shows comparison between the experimental and predicted collector's efficiency against radiation. The visual comparison of the experimental and ANN model collector's efficiency values, showed that the efficiency predicted by ANN model matched better with the measured. Hence, the visual checking of experimental and predicted collector's efficiency confirms that the ANN model performed well. The scatter plot of predicted collector's efficiency against experimental collector's efficiency as shown on Fig. 5 revealed that there was strong relationship between the predicted collector's efficiency and experimental collector's efficiency with $R^2 = 0.8890$. The similar trend was observed in Fig.6 for the predicted and experimental collector's efficiency value against temperature of the fluid entering the system.

4. Conclusion

The artificial neural network prediction of flat plate collector's efficiency for desalination of water provided an excellent matching with the experimental values. ANN based model can be used with a high degree of accuracy and reliability, thus showing the model can be reasonably applied for predicting other collector's efficiency once the inputs are identified.

References

- Edeoja, A. O., Bam, S. A. and Edeoja, J. A. (2009), "Comparison of a Flat Plate Collector and a Manually – Tracking Concentrating Collector for Air Heating in Makurdi", *Journal of Science and Technology Research*, 8(2), , International Research and Development Institute, Uyo
- Kuhe, A. (2004), Comparative Study of Flat Plate Collectors, M. Eng. Thesis, University of Agriculture,

Makurdi, pp. 30.

Ikpambese, K.K., Tuleun, L.T & Ager, P. (2012). Artificial neural network prediction of compressibility and oil absorption of gasket produced from palm kernel fibres. *Journal of Engineering Research*, 17(3).

Adnan S., Erol A. & Mehmet O. (2005) Formulation based on artificial neural network of thermodynamic properties of ozone friendly refrigerant/absorbent couples. *Applied Thermal Engineering*, 25, 1808–1820.

Zhang C.L.(2005) Generalized correlation of refrigerant mass flow rate through adiabatic capillary tubes using artificial neural network. *International Journal of Refrigeration*, 28, 506–14

Lolas, S. & Olatunbosun, A. O. (2008); Prediction of vehicle reliability performance using artificial neural networks, *Expert System with Application*, 34, 2360-2368.

Yasar I. (2003) A new approach for the prediction of the heat transfer rate of the wire-on-tube type heat exchangers-use of an artificial neural network mode. *Applied thermal Engineering*, 23, 243-249.

George, O. G. (1980), "Flat plate and Non-concentrating Collectors", In Solar Energy Technology Handbook (part B), pp. 239.

Gundu, D.T. Ikpambese, K.K., Ashwe, A. (2013). Prediction of extrusion pressure and product deflection of lead alloy extrudes using artificial neural networks, *American Journal of Engineering Research*, 02(06), 25-33.

Dragan, A. (2010), Neural network prediction of brake friction materials wear, *Wear*, 268 pp 117-125.

Haghadadi, N., Zarei-Hanzaki, A., Khalesian, A.R., and Abedi, H.R. (2013). Artificial neural modeling to predict the hot deformation behavior of an A356 aluminium alloy. *Materials and Design*, 49, 386-391.

Mohanty, S., Madan K., Ashawani K. & Panda D.K (2013) Comparative valuation of numerical model and artificial neural network for simulating groundwater flow in Kathajodi-Surua inter-basin of Odisha, India. *Journal of Hydrology*, 495, 38-51

Quan, G.Z., Lv, W.Q., Mao, Y.P., Zhang, Y.W, and Zhou, J. (2013). Prediction of flow stress in a wide temperature for as-cast Ti-6Al-2Zr-1Mo-1V alloy by artificial neural network, *Materials and Design*. Vol.50 pp 51-61.

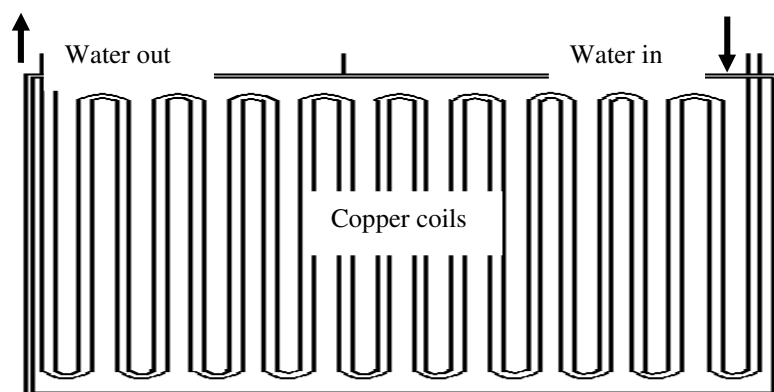


Fig. 1: Schematic Diagram of the System



Fig. 2: Photo of the Passive System

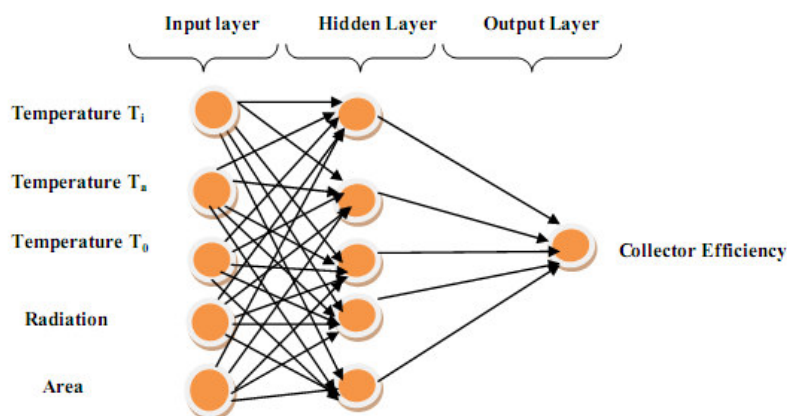


Fig.3: Neural network architecture used

Table 1: Set of input parameters used for training and testing.

Parameters	Test Data Set						
	Training data set ST ₁ -ST ₁₂	S _{p1}	S _{p2}	S _{p3}	S _{p4}	S _{p5}	S _{p6}
Atmospheric temperature (°C)	25 – 35	28.5	32	30	30.2	30	33.3
Temperature of the fluid entering the collector (°C)	30 – 42	30.3	34.2	32	31.5	32.3	36.1
Temperature of the fluid leaving the collector (°C)	35 – 70	46.4	44.2	41.8	47.7	61.5	62.1
Radiation (W/m ²)	200 – 450	252.3	388.3	227.5	285.8	365.8	421.7
Area of the collector (m ²)	1 – 3	2.31	2.31	2.31	2.31	2.31	2.31

Table 2: The experimental efficiency

Output parameter	S _{E1}	S _{E2}	S _{E3}	S _{E4}	S _{E5}	S _{E6}
Efficiency	0.57	0.58	0.56	0.58	0.57	0.57

Table 3: Predicted and experimental efficiency

Predicted	Experimental	Mean square error (MSE)	Correlation coefficient (R)	Nash-Scutcliffe efficiency (NSE)
0.57	0.57	-0.0000195	1.0000	1.0000
0.59	0.58	0.000000011	1.0000	0.9999
0.56	0.56	-.000000000139	1.0000	1.0000
0.58	0.58	0.0002912	1.0000	1.0000
0.57	0.57	0.0065103	1.0000	1.0000
0.57	0.57	0.000001340	1.0000	1.0000

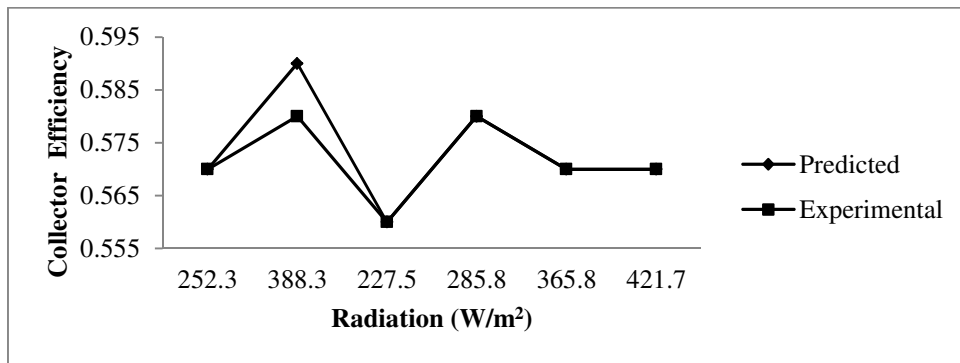


Fig. 4: Variation of collector efficiency against radiation

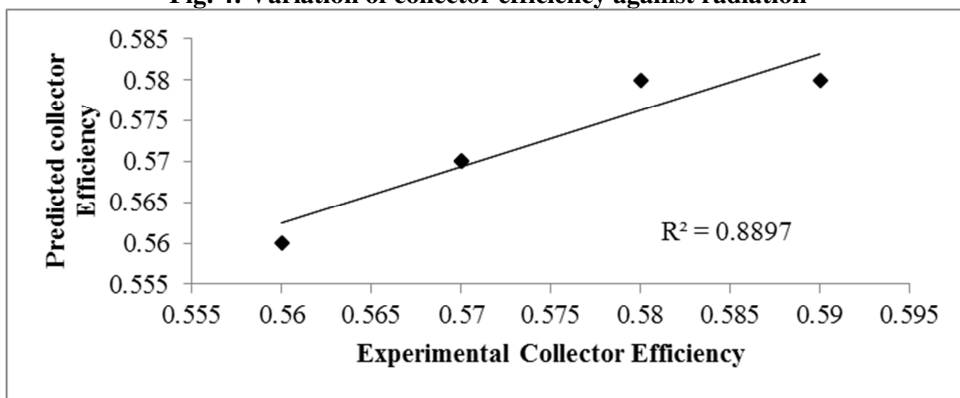


Fig. 5: Scatter plot of predicted and experimental collector efficiency

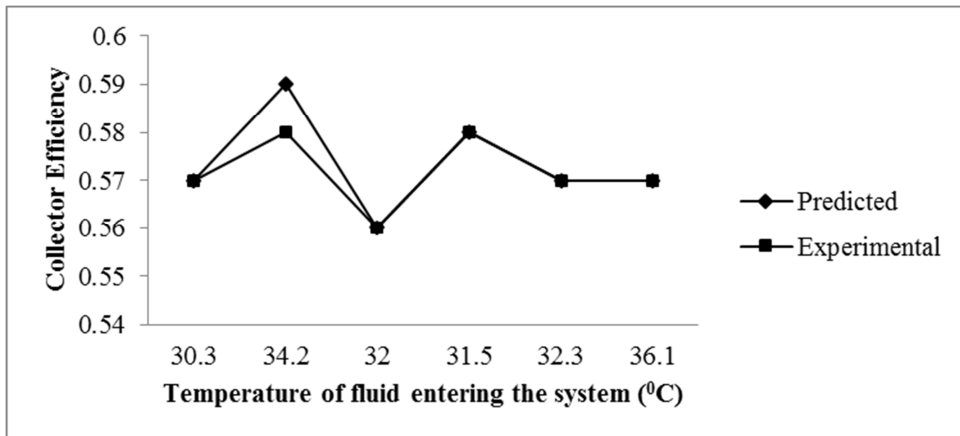


Fig. 6: Variation of collector efficiency against temperature of fluid entering the system.

The IISTE is a pioneer in the Open-Access hosting service and academic event management. The aim of the firm is Accelerating Global Knowledge Sharing.

More information about the firm can be found on the homepage:

<http://www.iiste.org>

CALL FOR JOURNAL PAPERS

There are more than 30 peer-reviewed academic journals hosted under the hosting platform.

Prospective authors of journals can find the submission instruction on the following page: <http://www.iiste.org/journals/> All the journals articles are available online to the readers all over the world without financial, legal, or technical barriers other than those inseparable from gaining access to the internet itself. Paper version of the journals is also available upon request of readers and authors.

MORE RESOURCES

Book publication information: <http://www.iiste.org/book/>

Academic conference: <http://www.iiste.org/conference/upcoming-conferences-call-for-paper/>

IISTE Knowledge Sharing Partners

EBSCO, Index Copernicus, Ulrich's Periodicals Directory, JournalTOCS, PKP Open Archives Harvester, Bielefeld Academic Search Engine, Elektronische Zeitschriftenbibliothek EZB, Open J-Gate, OCLC WorldCat, Universe Digital Library, NewJour, Google Scholar

